Parkinsonism and Related Disorders 104 (2022) 21–25

Contents lists available at ScienceDirect

Parkinsonism and Related Disorders

journal homepage: www.elsevier.com/locate/parkreldis

[^{18}F]FEOBV positron emission tomography may not be a suitable method to measure parasympathetic denervation in patients with Parkinson's disease

Jacob Horsager [a,b,*], Niels Okkels [a,b,c], Tatyana D. Fedorova [a,b], Karoline Knudsen [a], Casper Skjærbæk [a], Nathalie Van Den Berge [a,b], Jan Jacobsen [a], Ole Lajord Munk [a], Erik Hvid Danielsen [c], Dirk Bender [a], David J. Brooks [a,d], Per Borghammer [a,b]

[a] Department of Nuclear Medicine and PET, Aarhus University Hospital, Aarhus, Denmark
[b] Department of Clinical Medicine, Aarhus University, Aarhus, Denmark
[c] Department of Neurology, Aarhus University Hospital, Aarhus, Denmark
[d] Institute of Translational and Clinical Research, University of Newcastle Upon Tyne, UK

ARTICLE INFO

Keywords:
Parkinson's disease
Cholinergic
Parasympathetic
PET
[^{18}F]FEOBV

ABSTRACT

Introduction: The peripheral autonomic nervous system may be involved years before onset of motor symptoms in some patients with Parkinson's disease (PD). Specific imaging techniques to quantify the cholinergic nervous system in peripheral organs are an unmet need. We tested the hypothesis that patients with PD display decreased [^{18}F]FEOBV uptake in peripheral organs – a sign of parasympathetic denervation.

Methods: We included 15 PD patients and 15 age- and sex matched healthy controls for a 70 min whole-body dynamic positron emission tomography (PET) acquisition. Compartmental modelling was used for tracer kinetic analyses of adrenal gland, pancreas, myocardium, spleen, renal cortex, muscle and colon. Standard uptake values (SUV) at 60–70 min post injection were also extracted for these organs. Additionally, SUVs were also determined in the total colon, prostate, parotid and submandibular glands.

Results: We found no statistically significant difference of [^{18}F]FEOBV binding parameters in any organs between patients with PD and healthy controls, although trends were observed. The pancreas SUV showed a 14% reduction in patients ($P = 0.021$, not statistically significant after multiple comparison correction). We observed a trend towards lower SUVs in the pancreas, colon, adrenal gland, and myocardium of PD patients with versus without probable REM sleep behavior disorder.

Conclusion: [^{18}F]FEOBV PET may not be a sensitive marker for parasympathetic degeneration in patients with PD.

1. Introduction

Many patients with Parkinson's disease (PD) suffer from autonomic dysfunction. Several neuropathological studies have shown α-synuclein aggregates and prominent cell loss in autonomic structures, including up to a 50% cell loss in the dorsal motor nucleus of the vagus of deceased PD patients [1,2]. Braak and colleagues hypothesized that the initial α-synuclein pathology originates in the enteric nervous system and spreads retrogradely to the brainstem via vagal parasympathetic projections, and further rostrally to the substantia nigra [3]. This framework may explain why *some* patients have autonomic dysfunction several years prior to diagnosis (when motor symptoms first occur), why α-synuclein pathology can be found in intestinal samples up to 20 years prior to PD diagnosis, and why PD risk seems to be decreased in vagotomized patients [4–6]. In addition, preclinical research in animal models reproduce this stereotypical spreading pattern after intestinal preformed fibril injection [7].

However, not all PD patients conform to this paradigm. To resolve this controversy, it has been hypothesized that PD comprises two subtypes; a *body-first* subtype corresponding to Braak's hypothesis, and a *brain-first* subtype, where α-synuclein originates inside the brain and spreads in the opposite direction [8]. To study the validity of this model, imaging methods to assess peripheral autonomic degeneration are highly pertinent.

While imaging of the cardiac sympathetic nervous system is widely used both in research and to support a diagnosis of PD and DLB [9], the

* Corresponding author. Department of Nuclear Medicine and PET Aarhus University Hospital, Palle Juul-Jensens Boulevard 165, J220 8200 Aarhus N, Denmark.
E-mail address: jacobnls@rm.dk (J. Horsager).

https://doi.org/10.1016/j.parkreldis.2022.09.016
Received 17 June 2022; Received in revised form 22 September 2022; Accepted 25 September 2022
Available online 29 September 2022

parasympathetic nervous system has received less attention. Previous studies have utilized the positron emission tomography (PET) tracer 5-[^{11}C]-methoxy-donepezil ([^{11}C]donepezil) to quantify levels of acetylcholinesterase (AChE) binding in peripheral organs. In early-to-moderate stage disease PD patients, a significantly lower signal was found in the colon, small intestine, and pancreas [10,11]. In patients with isolated REM sleep behavior disorder (iRBD) (an early manifestation of body-first PD), similar results were found with significant uptake reductions in small intestine and colon [12]. *De novo* PD patients categorized as body-first PD (with premotor RBD) exhibited significantly lower colon [^{11}C]donepezil signal than brain-first PD (without RBD) [13]. Finally, surgically vagotomized patients also showed reduced colon signal, validating the role of this method to measure parasympathetic denervation [14]. Thus, [^{11}C]donepezil PET is a robust method to measure AChE density reductions in the gut of patients with PD. However, AChE is not a specific marker for cholinergic synapses since this enzyme is also produced in non-neuronal cells, and is observed in high concentration in brain areas without dense cholinergic innervation [15].

The PET tracer [^{18}F]fluoroethoxybenzovesamicol ([^{18}F]FEOBV) constitutes a recent advance in cholinergic imaging. [^{18}F]FEOBV binds to the vesicular acetylcholine transporter (VAChT), and is considered a very specific cholinergic marker, as it is almost exclusively located in synaptic vesicles of cholinergic neurons [16]. By using immunohistochemistry methods, VAChT has been identified in nerve terminals of several peripheral organs including the heart, gastrointestinal tract, adrenal medulla, prostate, pancreas, skeletal muscle motor endplate, salivary-, and lacrimal glands [17].

In this study, we hypothesized that patients with PD would display reduced [^{18}F]FEOBV binding in peripheral organs, reflecting parasympathetic (cholinergic) denervation.

2. Methods

2.1. Participants

We included 15 PD patients (time since diagnosis >4 years) and 15 healthy controls (HC). PD patients were diagnosed according to Movement Disorder Society's diagnostic criteria [9]. The HC data have been published previously [18]. Demographic and clinical data are presented in Table 1. Exclusion criteria were diabetes, gastrointestinal diseases, previous cancer, major surgery or radiation therapy to the head, thorax, or abdomen. Neurological and psychiatric disease were considered exclusion criteria in HC, and in patients if not related to PD. All participants provided written informed consent. The study was approved by the Science Ethical Committees of the Central Denmark Region (project number 1-10-72-201-18).

Table 1
Demographic and clinical information.

	HC	PD	P-value
Sample size *n*	15	15	
Sex *m/f*	8/7	9/6	0.99
Age	72.4 (7.9)	70.2 (7.3)	0.43
Time since diagnosis [years]	–	8.3 (2.5)	
UPDRS III (off)	–	32.2 (10.0)	
H&Y *II/III/IV (off)*	–	11/3/1	
LEDD [mg]	–	955 (383)	
BMI	24.8 (4.3)	24.7 (2.3)	0.98
OH, yes/no	1/14	6/9	0.08
Sniffin' sticks (olfaction)	12 (11–14)	6 (4–9)	**<0.0001**
MoCA	28.5 (1.1)	27.5 (1.8)	0.08
NMSS	9 (4–24)	53 (28–75)	**<0.0001**
SCOPA-AUT	7.2 (4.1)	16.4 (5.0)	**<0.0001**
RBDSQ	2 (2–4)	5 (4–9)	**0.0006**
RBDSQ, n > 5	1	7	
ROME III - nausea	0 (0–1)	0 (0–4)	0.25
ROME III - constipation	1 (0–4)	12 (3–25)	**0.0011**
Radiopaque markers, n	10 (8–24)	36 (24–39)	**0.009**
Colon transit time [days]	1.5 (1.3–2.9)	4.1 (2.9–4.4)	**0.009**
Colon volume [ml]	931.9 (384)	1285 (331)	**0.01**
Fasting gallbladder volume [ml]	29.8 (9.1)	44.7 (17.5)	**0.007**

Bold parameters mark significance. Parameters are presented as median (interquartile range) or mean (standard deviation). LEDD = Levodopa equivalent daily dose. OH = orthostatic hypotension.

2.2. [^{18}F]FEOBV PET/CT protocol

All images were generated on the same Siemens Biograph Vision 600 PET/CT scanner (*Siemens Healthcare, Erlangen, Germany*). The subjects were asked to abstain from eating for 6 h and drinking for 4 h before the scan. PD patients were allowed to take their medication with minimal water. All subjects were placed in supine position and injected with a bolus of approximately 200 MBq [^{18}F]FEOBV in a cubital vein. Simultaneously, a 6 min dynamic PET acquisition was initiated with a 26 cm field-of-view covering the heart and upper abdomen. Next, a whole-body PET recording was performed from 6 min to approximately 70 min using continuous bed motion. All PET images were reconstructed using TrueX, time-of-flight, 4 iterations, 5 subsets, 440 matrix, 2-mm Gaussian filtering, relative scatter correction, attenuation correction and were decay-corrected to the time of tracer injection. The final image voxel size was 1.65 × 1.65 × 3.0 mm^3. CT scans were performed before and after PET acquisition for attenuation correction; the latter included intravenous contrast enhancement for anatomical visualization of internal organs.

2.3. Volume-of-interest definition

For kinetic analyses, time-activity curves (TACs) from the dynamic PET images were extracted by sampling volumes-of-interest (VOI). The blood TAC was extracted using a circular region-of-interest (ROI) of 10 mm in diameter, placed in the lumen of the descending aorta, on 20 adjacent axial slices above the diaphragm. The colon signal was extracted through three steps. Part of the descending/transverse colon was outlined on the CT and this VOI was used as template for outlining the PET signal. Spill-in from surrounding organs was minimized by manually adjusting each ROI. The colon PET VOI activity was then normalized to the volume from the CT VOI. This volume was corrected for air content by subtracting an isocontour VOI of −300 Hounsfield Units. The adrenal gland TAC was obtained by sampling the whole gland PET signal and normalizing it to the CT volume. ROIs with a width of 8 mm were outlined in the hottest area for the pancreas (body and tail), left ventricular myocardium, spleen, and renal cortex using an 8 mm size brush on six adjacent axial slices. Muscle TACs were obtained by placing circular ROIs (10 mm diameter) in back muscle on 20 adjacent slices. Influence of movement artefacts was reduced by adjusting all VOIs separately to the PET signal on each individual PET frame. Due to gastric- and biliary tracer secretion, it was not possible to obtain meaningful data from the stomach, small intestine and head of pancreas.

For static analyses, the SUV was extracted from a summed whole-body image 60–70 min post injection. Here, the same approach was used for the pancreas, myocardium, adrenal gland, and total colon. The total colon SUV was corrected for colon volume using linear regression. In the prostate, central ROIs were placed on 6 adjacent slices with a diameter of 15 mm. The entire PET signals from the parotid- and submandibular glands were outlined and normalized to the CT-derived anatomical volumes. The lacrimal glands were sampled by placing three axial circular ROIs of 6 mm in diameter, surrounding the hottest area of the gland. Estimates from paired organs are presented as mean of right and left.

Colon and fasting gallbladder volumes were assessed by outlining the entire organ on the CT image. Colon volume was corrected for gender. Colon transit time was assessed by radiopaque marker method. In brief, 10 radiopaque markers are ingested every morning for 6 days prior to an

abdominal CT scan. The number of retained markers is used to calculate the colon transit time.

All analyses were performed using PMOD 4.0 (*Zürich, Switzerland*). VOI examples have been previously presented [18].

2.4. Kinetic modelling

We used a one-tissue compartment model, as this model gives the most robust fits of [^{18}F]FEOBV data in peripheral organs [18]. This model yields the kinetic parameters K_1 [ml/ccm/min] and k_2 [1/min], from which the total volume-of-distribution can be calculated ($V_t = K_1/k_2$ [ml/ccm]). All fits included unconstrained estimates of fractional blood volume (V_0) and time delay. We used the image-derived time--activity curve from the aortic lumen as the input function (see above). This input function was corrected for tracer binding to red blood cells, hematocrit, and metabolization of parent [^{18}F]FEOBV. The latter was assessed by drawing venous blood samples at 5, 15, 30, 45, and 60 min during PET acquisition, as previously described [18]. Due to missing data for some individuals, separate population metabolite-correction curves were generated for the HC and PD patients (**Supplementary Fig. 1**).

2.5. Statistics

Normality was investigated by visual inspection of QQ-plots and histograms. T-test or Mann Whitney *U* test was used for comparative analyses. The strength of the linear association between V_t and SUV were explored using Pearson product moment correlation coefficients. Holm-Bonferroni method was used to control for multiple comparison. All statistical analyses were performed with GraphPad Prism 7.0 and Stata 13.1.

3. Results

Patients with PD did not differ from HC on demographic parameters and expected clinical differences were observed (Table 1). Patients with PD more often had orthostatic hypotension, hyposmia, other non-motor symptoms, and a higher score on RBDSQ. In addition, PD patients showed objective signs of colon and gallbladder dysfunction (increased colon volume, colon transit time, and fasting gallbladder volume).

[^{18}F]FEOBV accumulation was observed in organs with known cholinergic innervation. Kinetic analyses using the one-tissue compartment model revealed a slightly lower median V_t of pancreas (HC: 24.3 ml/ccm vs. PD: 21.9 ml/ccm) and a higher median V_t of skeletal muscle in patients with PD (HC: 4.2 ml/ccm vs. PD: 5.1 ml/ccm), but these differences were not statistically significant (Table 2). Of note, kinetic analyses using Logan plots were also performed and generated similar V_t results (data not shown). We found a marginally faster rate of [^{18}F]FEOBV metabolism in PD patients, with a 6% difference in parent tracer level after 60 min (30% in HC vs 24% in PD) (Supplementary Fig. 1).

SUVs extracted from a static whole-body PET image 60–70 min post injection are presented in Table 3. We found a 14% lower median pancreas SUV in PD patients, but the difference was not statistically significant after multiple comparison correction (Fig. 1). The median skeletal muscle SUV was 31% higher in PD patients than HC. No significant differences were observed in other organs (Table 3). In a subgroup analysis, the PD group was categorized based on RBDSQ into a probable RBD group (PD + pRBD; RBDSQ $\geq$6) and no RBD group (PD-pRBD; RBDSQ $\leq$5). We observed trends towards lower [^{18}F]FEOBV SUV in total colon, pancreas, adrenal gland, and myocardium in the PD + pRBD, but none reached statistical significance (Supplementary Table 1). There was no difference in adrenal gland SUV between patients with and without orthostatic hypotension.

We found significant correlations between V_t and SUV in pancreas ($r = 0.8$, $P < 0.0001$) (Fig. 1), colon ($r = 0.65$, $P = 0.0001$), myocardium ($r = 0.57$, $P = 0.0009$), adrenal gland ($r = 0.51$, $P = 0.004$), and muscle ($r = 0.7$, $P < 0.0001$) across study groups. They remained significant when groups were analyzed individually, except for the adrenal gland where only trends were observed (HC: $r = 0.46$, $P = 0.09$, PD: $r = 0.51$, $P = 0.052$).

Table 3
SUV of peripheral organs.

60–70 min	HC	PD	P-value
Total colon[a]	1.02 (0.27)	0.92 (0.15)	0.20
Pancreas	6.77 (5.9–8.44)	5.81 (5.34–6.48)	**0.021**
Adrenal gland	8.76 (1.54)	7.76 (1.67)	0.10
Myocardium	6.37 (5.46–7.44)	6.78 (5.52–7.53)	0.46
Parotid gland	4.45 (0.81)	4.08 (0.78)	0.21
Submandibular gland	4.06 (0.90)	3.65 (0.93)	0.25
Lacrimal gland	1.99 (0.62)	2.00 (0.43)	0.95
Prostate	1.65 (0.45)	1.50 (0.24)	0.39
Muscle	1.13 (0.94–1.28)	1.48 (1.26–1.9)	**0.016**

[a] Total colon SUV was corrected for colon volume by linear regression. Parameters are presented as mean (SD) or median (interquartile range). No differences were significant after multiple comparison correction.

4. Discussion

In this study, we tested the hypothesis that the [^{18}F]FEOBV signal is reduced in peripheral organs of patients with moderate stage PD with presumed parasympathetic denervation. In kinetic analyses of dynamic [^{18}F]FEOBV data, we found no significant differences between PD patients and healthy controls in V_t of any organ. The image-derived input functions for these analyses were corrected for peripheral metabolism using a population-derived curve (for each group) due to missing data for some individuals. In addition, we were unable to determine the fraction of [^{18}F]FEOBV binding to plasma proteins (free fraction). The uncertainty introduced by these circumstances may have resulted in increased data variance and therefore a failure to reject the null hypothesis in this study.

We found moderate-to-strong correlations between V_t and SUV extracted from a static image 60–70 min post injection in most organs, particularly in the pancreas, adrenal gland, colon, myocardium, and skeletal muscle. Therefore, a static PET image after 60–70 min with SUV

Table 2
Kinetic parameters.

	K_1 [ml/ccm/min]		k_2 [1/min]		V_t [ml/ccm]	
	HC	PD	HC	PD	HC	PD
Pancreas	1.00 (0.77–1.17)	0.81 (0.66–1.31)	0.038 (0.033–0.046)	0.046 (0.031–0.048)	24.3 (18.5–31.6)	21.9 (17.4–27.1)
Renal cortex	1.73 (1.25–1.84)	1.54(1.40–1.74)	0.25 (0.23–0.27)	0.25 (0.20–0.30)	6.06 (5.25–7.76)	6.13 (5.38–7.61)
Spleen	1.39 (1.20–1.72)	1.18 (1.05–1.49)	0.12 (0.10–0.16)	0.14 (0.11–0.15)	9.72 (9.15–12.7)	9.43 (8.89–1097)
Myocardium	0.63 (0.54–0.78)	0.66 (0.57–0.72)	0.027 (0.023–0.036)	0.029 (0.023–0.035)	24.3 (17.8–32.0)	23.6 (19.2–29.4)
Muscle	0.049 (0.04–0.09)	0.12 (0.08–0.22)	0.012 (0.010–0.016)	0.022 (0.015–0.038)	4.20 (3.73–5.26)	5.09 (4.31–5.95)
Adrenal gland	0.59 (0.39–0.62)	0.51 (0.46–0.62)	0.019 (0.007–0.021)	0.019 (0.014–0.021)	33.1 (30.0–55.9)	31.6 (26.3–33.5)
Colon	0.078 (0.063–0.1)	0.063 (0.053–0.073)	0.029 (0.021–0.041)	0.026 (0.021–0.035)	2.64 (1.94–3.51)	2.51 (1.97–3.01)

All parameters are presented as median (interquartile range). No statistically significant differences were observed between PD patients and HC.

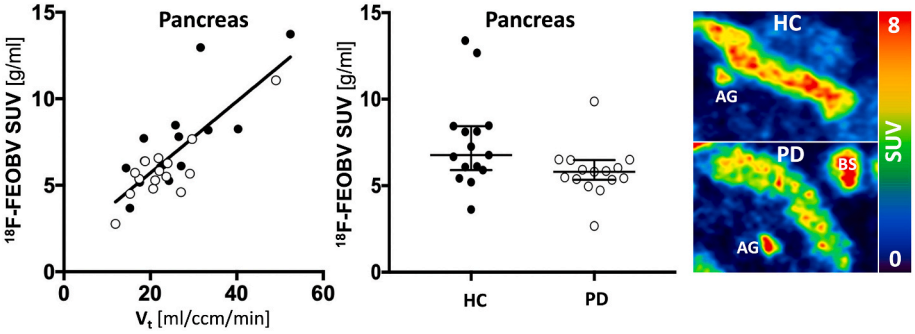

Figure 1. Left: correlation between SUV and volume-of-distribution (V_t) in pancreas ($r = 0.8$, $P < 0.0001$). The correlation was significant in both HC and PD individually. Middle: Lower pancreas SUV was seen in PD compared to HC ($P = 0.021$), but the difference did not survive multiple comparison correction. Increased variance was observed in the HC group. Error bars represent median and interquartile range. Right: Representative SUV images of pancreas in a HC (top) and a patient with PD (bottom). AG = adrenal gland; BS = bile in small intestine.

calculation may be sufficient to obtain a reliable estimate of VAChT density in these organs.

In the pancreas, we found a small (14%) reduction in median SUV, but the difference was not statistically significant after multiple comparison correction. However, the result is in line with a previous [^{11}C]donepezil PET study in early-moderate PD patients showing a 22% reduction in pancreas AChE density [10]. In contrast, another [^{11}C]donepezil PET study failed to show difference between early PD patients and HC [11]. Two circumstances may have limited our ability to detect pancreatic cholinergic denervation in PD patients. First, the head of pancreas contains most vagal parasympathetic projections [19], but we were unable to extract meaningful data from that area due to biliary secretion of [^{18}F]FEOBV. Instead, we analyzed the body and tail. Second, human pancreatic alpha and delta-cells also express VAChT [20], but these are unlikely to be affected in patients with PD.

The mean total colon SUV was approximately 10% lower in PD patients than HC, but the difference was not statistically significant. This was rather unexpected, as previous studies with [^{11}C]donepezil consistently showed reduced signal in both PD and iRBD patients [11–13]. Previous immunohistochemistry studies have failed to show loss of enteric neurons (including cholinergic) in PD patients [21,22]. This suggests that reduced AChE density, measured by [^{11}C]donepezil PET, reflects, at least in part, parasympathetic denervation. However, other mechanisms may cause the discrepancy between [^{11}C]donepezil and [^{18}F]FEOBV PET. First, α-synuclein pathology is present in intestinal tissue samples of patients with PD [23]. Second, α-synuclein in human colon samples selectively co-localizes with VAChT; 71% of VAChT-labelled neurons stain for α-synuclein compared to only 10% of other neuronal types [24]. Therefore, it is probable that intestinal cholinergic neurons are "sick, but not dead", a principle described for catecholaminergic neurons in α-synucleinopathies, implying that nerve terminals are still present, but functional abnormalities result in reduced neurotransmitter release [25]. Similar mechanisms have not, to our knowledge, been described for cholinergic neurons in PD. However, one study in patients with Alzheimer's disease showed that AChE in the frontal lobe was reduced earlier in the disease course than choline acetyltransferase (ChAT) [26]. Since ChAT and VAChT show almost complete anatomical overlap [27], it could be speculated that in patients with PD, AChE is downregulated in dysfunctional enteric cholinergic neurons where there is little (or no) loss of synapses. This would cause prolonged neurotransmitter presence in the synaptic cleft, which is likely a desirable homeostatic mechanism in the face of cholinergic dysfunction. However, the putative regulation of AChE in neurodegenerative diseases has to our knowledge not been studied.

We found no significant difference in left ventricular myocardium SUV between groups. This was expected, as the dominating contributor to this signal probably is generated by cardiomyocyte-derived VAChT production [28], and hence not parasympathetic innervation.

In a subgroup analysis of PD patients based on RBDSQ scores we found trends towards lower SUV values in total colon, pancreas, and adrenal gland in patients with probable RBD, defined as RBDSQ $\geq$6 (Supplementary table 1). This fits well with the brain-first and body-first PD paradigm, since more body-first patients are expected in this group – despite the potentially low diagnostic accuracy of RBDSQ [29]. We previously showed that PD patients with RBD showed significantly lower [^{11}C]donepezil uptake compared to PD patients without RBD [13]. However, that study included a considerably larger sample of PD patients (37 in total) and employed gold standard video-polysomnography for RBD diagnosis. Thus, the limited differences between RBD-positive and -negative studies in the present study could be due to lack of statistical power and inaccurate RBD assessment.

The negative results in this study may not (only) have methodological origin, but could also reflect no or limited parasympathetic denervation in our PD cohort. Evidence for parasympathetic involvement in PD include neuropathological [1,2], epidemiological [6], and imaging studies [11–14]. An [^{18}F]dopamine PET study showed markedly decreased sympathetic innervation of the heart, but not in abdominal organs [30]. If this "cardioselectivity" also applies to the parasympathetic nervous system, it would explain why limited differences were observed in the present study, where the primary myocardial [^{18}F]FEOBV signal probably derives from the cardiomyocytes and not parasympathetic neurons [28]. In addition, it is unknown whether post-ganglionic parasympathetic neurons degenerate. Thus, further research is needed to understand how the parasympathetic nervous system is affected in PD.

This study has several limitations. Kinetic analyses were performed with an image-derived aortic lumen input function, modified by a population-based peripheral metabolite correction curve. This curve was generated from data with high statistical variance. We did not expect any differences between the groups in rate of peripheral tracer metabolism, but found a slightly faster metabolism in PD patients – probably caused by statistical noise. Therefore, compared to HC, we may have overestimated the V_t in PD patients. In addition, the free fraction was not determinable, which introduced an additional uncertainty in the kinetic analyses. Kinetic analyses were not performed blinded to clinical status, but all analyses on static images (yielding SUVs) were performed blinded to clinical status. Due to the high lipophilicity, [^{18}F]FEOBV will remain diffusely in tissues for an unknown period. This is non-displaceable tracer uptake and does therefore not represent VAChT density. Also, non-specific binding has not been assessed for [^{18}F]FEOBV in internal organs. Another cholinergic PET tracer, [^{11}C]donepezil, generally display low non-specific binding in internal organs (3–17%) [31]. However, this is not necessarily translatable to [^{18}F]FEOBV. Secretion was overt from the stomach, and was thus omitted from kinetic modelling. However, other excretory organs, such as colon, pancreas, and salivary glands may also secrete the tracer. Tracer in the lumen of e.g. the pancreatic duct would contribute to the [^{18}F]FEOBV signal, and severely undermine the interpretation of V_t and SUV as measures of VAChT density. However, careful inspection of the dynamic images did not reveal overt secretion. Still, these limitations may have caused our inability to show between-group differences and probably disqualifies [^{18}F]FEOBV as a measure of cholinergic neurons in internal

organs.

To conclude, we found reduced [^{18}F]FEOBV SUVs in the pancreas of PD patients, but the difference did not survive multiple comparison correction. No difference was found in V_t computed from kinetic analyses. This study suggests that [^{18}F]FEOBV PET may not be a sensitive marker for cholinergic degeneration in peripheral organs of PD patients.

Funding sources

The study was funded by Lundbeck Foundation [grant number: R190-2014-4183] and Aase og Ejnar Danielsens Fond [project nr. 36456]. Funding sources had no role in the study.

Data availability

Data will be provided by the corresponding author upon reasonable request.

Financial disclosures

The study was funded by Lundbeck Foundation [grant number: R190-2014-4183] andAase og Ejnar Danielsens Fond [project nr. 36456]. Funding sources had no role in the study.

Ethics

The study was approved by the Science Ethical Committees of the Central Denmark Region (project number 1-10-72-201-18).

Declaration of competing interest

The authors have no conflicts of interests to declare.

Appendix A. Supplementary data

Supplementary data to this article can be found online at https://doi.org/10.1016/j.parkreldis.2022.09.016.

References

[1] S. Orimo, E. Ghebremedhin, E. Gelpi, Peripheral and central autonomic nervous system: does the sympathetic or parasympathetic nervous system bear the brunt of the pathology during the course of sporadic PD? Cell Tissue Res. 373 (1) (2018) 267–286.
[2] W.P. Gai, P.C. Blumbergs, L.B. Geffen, W.W. Blessing, Age-related loss of dorsal vagal neurons in Parkinson's disease, Neurology 42 (11) (1992) 2106–2111.
[3] C.H. Hawkes, K. Del Tredici, H. Braak, Parkinson's disease: a dual-hit hypothesis, Neuropathol. Appl. Neurobiol. 33 (6) (2007) 599–614.
[4] S.M. Fereshtehnejad, C. Yao, A. Pelletier, J.Y. Montplaisir, J.F. Gagnon, R. B. Postuma, Evolution of prodromal Parkinson's disease and dementia with Lewy bodies: a prospective study, Brain 142 (7) (2019) 2051–2067.
[5] M.G. Stokholm, E.H. Danielsen, S.J. Hamilton-Dutoit, P. Borghammer, Pathological alpha-synuclein in gastrointestinal tissues from prodromal Parkinson disease patients, Ann. Neurol. 79 (6) (2016) 940–949.
[6] E. Svensson, E. Horvath-Puho, R.W. Thomsen, J.C. Djurhuus, L. Pedersen, P. Borghammer, H.T. Sorensen, Vagotomy and subsequent risk of Parkinson's disease, Ann. Neurol. 78 (4) (2015) 522–529.
[7] N. Van Den Berge, N. Ferreira, H. Gram, T.W. Mikkelsen, A.K.O. Alstrup, N. Casadei, P. Tsung-Pin, O. Riess, J.R. Nyengaard, G. Tamguney, P.H. Jensen, P. Borghammer, Evidence for bidirectional and trans-synaptic parasympathetic and sympathetic propagation of alpha-synuclein in rats, Acta Neuropathol. 138 (4) (2019) 535–550.
[8] P. Borghammer, N. Van Den Berge, Brain-first versus gut-first Parkinson's disease: a hypothesis, J. Parkinsons Dis. 9 (s2) (2019) S281–S295.
[9] R.B. Postuma, D. Berg, M. Stern, W. Poewe, C.W. Olanow, W. Oertel, J. Obeso, K. Marek, I. Litvan, A.E. Lang, G. Halliday, C.G. Goetz, T. Gasser, B. Dubois, P. Chan, B.R. Bloem, C.H. Adler, G. Deuschl, MDS clinical diagnostic criteria for Parkinson's disease, Mov. Disord. 30 (12) (2015) 1591–1601.
[10] T. Gjerloff, T. Fedorova, K. Knudsen, O.L. Munk, A. Nahimi, S. Jacobsen, E. H. Danielsen, A.J. Terkelsen, J. Hansen, N. Pavese, D.J. Brooks, P. Borghammer, Imaging acetylcholinesterase density in peripheral organs in Parkinson's disease with 11C-donepezil PET, Brain 138 (Pt 3) (2015) 653–663.
[11] T.D. Fedorova, L.B. Seidelin, K. Knudsen, A.C. Schacht, J. Geday, N. Pavese, D. J. Brooks, P. Borghammer, Decreased intestinal acetylcholinesterase in early Parkinson disease: an (11)C-donepezil PET study, Neurology 88 (8) (2017) 775–781.
[12] K. Knudsen, T.D. Fedorova, A.K. Hansen, M. Sommerauer, M. Otto, K.B. Svendsen, A. Nahimi, M.G. Stokholm, N. Pavese, C.P. Beier, D.J. Brooks, P. Borghammer, In-vivo staging of pathology in REM sleep behaviour disorder: a multimodality imaging case-control study, Lancet Neurol. 17 (7) (2018) 618–628.
[13] J. Horsager, K.B. Andersen, K. Knudsen, C. Skjaerbaek, T.D. Fedorova, N. Okkels, E. Schaeffer, S.K. Bonkat, J. Geday, M. Otto, M. Sommerauer, E.H. Danielsen, E. Bech, J. Kraft, O.L. Munk, S.D. Hansen, N. Pavese, R. Goder, D.J. Brooks, D. Berg, P. Borghammer, Brain-first versus body-first Parkinson's disease: a multimodal imaging case-control study, Brain 143 (10) (2020) 3077–3088.
[14] T.D. Fedorova, K. Knudsen, B. Hartmann, J.J. Holst, F. Viborg Mortensen, K. Krogh, P. Borghammer, In vivo positron emission tomography imaging of decreased parasympathetic innervation in the gut of vagotomized patients, Neuro Gastroenterol. Motil. 32 (3) (2020), e13759.
[15] S.A. Greenfield, A noncholinergic action of acetylcholinesterase (AChE) in the brain: from neuronal secretion to the generation of movement, Cell. Mol. Neurobiol. 11 (1) (1991) 55–77.
[16] G.K. Mulholland, D.M. Wieland, M.R. Kilbourn, K.A. Frey, P.S. Sherman, J. E. Carey, D.E. Kuhl, [18F]fluoroethoxy-benzovesamicol, a PET radiotracer for the vesicular acetylcholine transporter and cholinergic synapses, Synapse 30 (3) (1998) 263–274.
[17] U. Arvidsson, M. Riedl, R. Elde, B. Meister, Vesicular acetylcholine transporter (VAChT) protein: a novel and unique marker for cholinergic neurons in the central and peripheral nervous systems, J. Comp. Neurol. 378 (4) (1997) 454–467.
[18] J. Horsager, N. Okkels, N. Van Den Berge, J. Jacobsen, A. Schact, O.L. Munk, K. Vang, D. Bender, D.J. Brooks, P. Borghammer, In vivo vesicular acetylcholine transporter density in human peripheral organs: an [(18)F]FEOBV PET/CT study, EJNMMI Res. 12 (1) (2022) 17.
[19] H.R. Berthoud, N.R. Carlson, T.L. Powley, Topography of efferent vagal innervation of the rat gastrointestinal tract, Am. J. Physiol. 260 (1 Pt 2) (1991) R200–R207.
[20] R. Rodriguez-Diaz, R. Dando, M.C. Jacques-Silva, A. Fachado, J. Molina, M. H. Abdulreda, C. Ricordi, S.D. Roper, P.O. Berggren, A. Caicedo, Alpha cells secrete acetylcholine as a non-neuronal paracrine signal priming beta cell function in humans, Nat. Med. 17 (7) (2011) 888–892.
[21] D.M. Annerino, S. Arshad, G.M. Taylor, C.H. Adler, T.G. Beach, J.G. Greene, Parkinson's disease is not associated with gastrointestinal myenteric ganglion neuron loss, Acta Neuropathol. 124 (5) (2012) 665–680.
[22] F. Giancola, F. Torresan, R. Repossi, F. Bianco, R. Latorre, A. Ioannou, M. Guarino, U. Volta, P. Clavenzani, M. Mazzoni, R. Chiocchetti, F. Bazzoli, R.A. Travagli, C. Sternini, R. De Giorgio, Downregulation of neuronal vasoactive intestinal polypeptide in Parkinson's disease and chronic constipation, Neuro Gastroenterol. Motil. 29 (5) (2017).
[23] K. Wakabayashi, H. Takahashi, S. Takeda, E. Ohama, F. Ikuta, Parkinson's disease: the presence of Lewy bodies in Auerbach's and Meissner's plexuses, Acta Neuropathol. 76 (3) (1988) 217–221.
[24] D.F. Sharrad, E. de Vries, S.J. Brookes, Selective expression of alpha-synuclein-immunoreactivity in vesicular acetylcholine transporter-immunoreactive axons in the Guinea pig rectum and human colon, J. Comp. Neurol. 521 (3) (2013) 657–676.
[25] D.S. Goldstein, The "Sick-but-not-Dead" phenomenon applied to catecholamine deficiency in neurodegenerative diseases, Semin. Neurol. 40 (5) (2020) 502–514.
[26] S.T. DeKosky, R.E. Harbaugh, F.A. Schmitt, R.A. Bakay, H.C. Chui, D.S. Knopman, T.M. Reeder, A.G. Shetter, H.J. Senter, W.R. Markesbery, Cortical biopsy in Alzheimer's disease: diagnostic accuracy and neurochemical, neuropathological, and cognitive correlations, Intraventricular Bethanecol. Study Group, Ann. Neurol. 32 (5) (1992) 625–632.
[27] C.A. Altar, M.R. Marien, [3H]vesamicol binding in brain: autoradiographic distribution, pharmacology, and effects of cholinergic lesions, Synapse 2 (5) (1988) 486–493.
[28] Y. Kakinuma, T. Akiyama, T. Sato, Cholinoceptive and cholinergic properties of cardiomyocytes involving an amplification mechanism for vagal efferent effects in sparsely innervated ventricular myocardium, FEBS J. 276 (18) (2009) 5111–5125. 29.
[29] K. Stiasny-Kolster, F. Sixel-Doring, C. Trenkwalder, M. Heinzel-Gutenbrunner, K. Seppi, W. Poewe, B. Hogl, B. Frauscher, Diagnostic value of the REM sleep behavior disorder screening questionnaire in Parkinson's disease, Sleep Med. 16 (1) (2015) 186–189.
[30] G. Lamotte, C. Holmes, P. Sullivan, A. Lenka, D.S. Goldstein, Cardioselective peripheral noradrenergic deficiency in Lewy body synucleinopathies, Ann. Clin. Transl. Neurol. 7 (12) (2020) 2450–2460.
[31] T. Gjerloff, S. Jakobsen, A. Nahimi, O.L. Munk, D. Bender, A.K. Alstrup, K.H. Vase, S.B. Hansen, D.J. Brooks, P. Borghammer, In vivo imaging of human acetylcholinesterase density in peripheral organs using 11C-donepezil: dosimetry, biodistribution, and kinetic analyses, J. Nucl. Med. 55 (11) (2014) 1818–1824.